An Oligomeric Protein Is Imported into Peroxisomes In Vivo

James A. McNew and Joel M. Goodman

Department of Pharmacology, University of Texas Southwestern Medical Center, Dallas, Texas 75235-9041

Abstract. The mechanism of translocation of peroxisomal proteins from the cytoplasm into the matrix is largely unknown. We have been studying this problem in yeast. We show that the peroxisomal targeting sequences SKL or AKL, with or without a spacer of nine glycines (G9), are sufficient to target chloramphenicol acetyltransferase (CAT) to peroxisomes of *Saccharomyces cerevisiae* in vivo. The mature form of CAT is a homotrimer, and complete trimerization of CAT was found to occur within a few minutes of synthesis. In contrast, import, measured by immunoelectron microscopy and organellar fractionation, occurred over several hours. To confirm that import of preassembled CAT trimers was occurring, we co-expressed CAT-G9-AKL with CAT lacking a peroxisomal targeting sequence but containing a hemagglutinin-derived epitope tag (HA-CAT). We found that HA-CAT was not imported unless it was co-expressed with CAT-G9-AKL. Both proteins were released from the organelles under mild conditions (pH 8.5) that released other matrix proteins, indicating that import had occurred. These results strongly suggested that HA-CAT was imported as a heterotrimer with CAT-G9-AKL. The process of oligomeric import also occurs in animal cells. When HA-CAT was co-expressed with CAT-G9-AKL in CV-1 cells, HA-CAT co-localized with peroxisomes but was cytoplasmic when expressed alone. It is not clear whether the import of globular proteins into peroxisomes occurs through peroxisomal membrane pores or involves membrane internalization. Both possibilities are discussed.

M ANY proteins that are synthesized in the cytoplasm are destined for organelles and must cross at least one membrane en route to their final destination. Fully folded proteins are not competent for export from the cytoplasm in prokaryotes (Randall and Hardy, 1986; Wickner et al., 1991), nor for import into mitochondria (Eilers and Schatz, 1986; Chen and Douglas, 1987), or into the lumen of the endoplasmic reticulum in eukaryotes (Sanz and Meyer, 1988). Cytoplasmic chaperones are proposed to maintain proteins in an unfolded translocation-competent state (Deshaies et al., 1988; Hendrick and Hartl, 1993) until encountering the *Escherichia coli* inner envelope, the mitochondrial outer membrane, or the endoplasmic reticulum. Folding later occurs within the organelles after translocation has begun. While the import of proteins into chloroplasts was thought to require unfolded substrates as well, recent evidence suggests that this might not be correct (America et al., 1994).

In contrast to these organelles, the nuclear envelope contains pore complexes through which folded proteins of less than 50,000 kD can freely diffuse (Bonner, 1978). Larger proteins are imported through the nuclear pores by an active mechanism that requires *cis*-acting nuclear targeting sequences and ATP (Dingwell et al., 1982; Newmeyer et al., 1986; Silver, 1991).

Much less is known about import into peroxisomes. Many peroxisomal proteins contain the sequence SKL or a close variant of this tripeptide at their extreme carboxy termini (de Hoop and Ab, 1992). This motif has been termed PTS1 (peroxisomal targeting signal 1). Peroxisomal targeting signal 1 (PTS1)[1] has been shown to vary slightly according to species. In mammalian cells, allowable substitutions are A or C for S, R or H for K, and M for L (Gould et al., 1989), although these variants sort with different efficiencies (Swinkels et al., 1992). In the yeast *Hansenula polymorpha*, the sequences ARF and NKL can function (Hansen et al., 1992); in *Candida tropicalis* AKI can serve as a PTS1 (Aitchison et al., 1991). In trypanosomal glycosomes, a sequence similar to that of mammalian cells is recognized, although S is allowed at the second position (SSL) and M at the last position (SKM) (Blattner et al., 1992). The peroxisomal targeting requirements for *Saccharomyces cerevisiae*, however, are not so clear. The attachment of SKL to the carboxy terminus of dihydrofolate reductase (DHFR) did not

---

Address all correspondence to J. Goodman, Department of Pharmacology, University of Texas Southwestern Medical Center, 5323 Harry Hines Blvd., Dallas, TX 75235-9041. Ph.: (214) 648-2359. Fax: (214) 648-2994.

---

permit localization to peroxisomes in *S. cerevisiae*, suggesting that recognition of this motif may be more complex in this yeast (Distel et al., 1992; Kragler et al., 1993).

A second type of targeting signal, termed PTS2, is found on amino terminal extensions of 3-ketoacyl CoA thiolase (Swinkels et al., 1991) and plant malate dehydrogenase (Gietl, 1990). Several peroxisomal matrix proteins, however, do not contain either PTS1 or PTS2. The mechanism for their targeting is unknown.

Peroxisomal proteins are imported posttranslationally from cytoplasm to matrix (Lazarow and Fujiki, 1985). Most matrix proteins are oligomeric. A comparison of the kinetics of import and oligomerization has been performed in a few cases. Thus, catalase in rat liver (Lazarow and de Duve, 1973), and alcohol oxidase in the yeast *Candida boidinii* (Goodman et al., 1984), became oligomeric within several minutes, concomitant with their association with organelles. A recent study of catalase biosynthesis in normal human skin fibroblasts, however, showed that tetramerization occurred shortly after synthesis (monomers were not detected) while incorporation into peroxisomes occurred over several hours (Middelkoop et al., 1993). Thus, oligomerization and import are not necessarily coupled.

This report describes the sorting of chloramphenicol acetyltransferase (CAT)-PTS1 chimeras to peroxisomes in *S. cerevisiae*. We show that AKL or SKL is sufficient to target CAT to these organelles in vivo. Furthermore, we present evidence that CAT is imported as a folded trimeric protein. We present three possible mechanistic models to explain our data.

Materials and Methods

Strains and Culture Conditions

S. cerevisiae strain MMY011 (*MATα ade 2-1 his3-11,15 leu2-3,112 trp1-1 ura3-1 can1-100* Ole⁺) (McCammon et al., 1990) was used throughout this study. Routine molecular biology was performed according to Sambrook (Sambrook et al., 1989). *E. coli* strain TG-1 (F' *traD36 lacIq Δ[lacZ]M15 proA+B+/supE Δ[hsdM-mcrB]5* [$r_k^- m_k^-$McrB⁻] *thi Δ(lac-proAB)*) was used for standard manipulations. CJ236 (F' *catf*=pCJ105; M13ˢ Cmʳ]/*dut ung1 thi-1 relA1 spoT1 mcrA*) was used for oligonucleotide-directed mutant enrichment. Transformed yeast strains were maintained on synthetic dextrose (SD) plates (0.67% Yeast Nitrogen Base without amino acids [Difco Labs, Detroit, MI] and 2% glucose), with amino acid and base supplements as needed. Routine peroxisomal induction and plasmid expression were accomplished by inoculating 250 ml of synthetic glycerol-dextrose (SGd) (containing 3% glycerol and 0.1% glucose) from an SD plate. The cells were grown for approximately 2 d to an OD$_{600}$ of 2–3. 250 OD$_{600}$ U of cell were transferred to a new flask and "boosted" with 1× YP (1% yeast extract, 2% peptone) for 4 h. The cells were then collected by centrifugation at 7,500 *g* for 10 min and resuspended at a final concentration of 1 OD$_{600}$ U/ml in semi-synthetic oleate medium (containing 0.05% yeast extract and 0.1% oleic acid; McCammon et al., 1990) supplemented with amino acids and bases as required. Cells were incubated in oleate medium for 12–15 h, then galactose was added to 0.1%. They were then harvested 24 h after galactose addition (except where noted in the figure legends).

Preparation of Spheroplasts and Organelle Fractionation

Cells were converted to spheroplasts (McCammon et al., 1990) using Zymolyase 100T (ICN Biomedicals, Irvine, CA) at 0.5 μg/OD$_{600}$ U of cells. All subsequent steps were performed at 0–4°C. The spheroplasts were harvested by centrifugation at 7,500 *g* for 10 min and resuspended in 2 ml of 1 M SMA (1 M sorbitol, 5 mM 2-[*N*-morpholinoethanesulfonate], pH 5.5, and 0.2 mM [4-{2-aminoethyl} benzenesulfonylfluoride HCl]). Osmotic ly-

sis was achieved by adding 6 ml of 0.25 M SMA (0.25 M sorbitol, 5 mM 2-[*N*-morpholinoethanesulfonate], pH 5.5, and 0.2 mM [4-{2-aminoethyl}-benzenesulfonylfluoride HCl]). Lysis was ~70–80% as determined by microscopic analysis. The lysate was returned to the original osmolarity by the addition of 6 ml of 1.75 M SMA (containing 1.75 M sorbitol). The lysate was centrifuged at 1,000 *g* for 5 min to remove unbroken cells, nuclei, and other large particles. This low-speed supernatant was carefully removed and the pellet was re-extracted with 2 ml of 1 M SMA to recover trapped organelles. After centrifugation, the two supernatants were combined and centrifuged at 1,000 *g* again. The combined low-speed supernatants were centrifuged at 25,000 *g* for 25 min. The pellet from this spin ("crude organelles") was resuspended in 200 μl of 1 M SMA. For analysis of crude organellar supernatants and pellets, 2–3% of each supernatant and pellet were precipitated with TCA, and 0.5–0.6% of each were analyzed by SDS-PAGE. Peroxisomes and mitochondria in this fraction were separated in a sucrose gradient as described (McCammon et al., 1990) with the following modifications: 4-ml sucrose gradients were used, and they were centrifuged at 201,000 *g*$_{ave}$ for 5.5 h in an SW60 rotor. For the experiment described in Fig. 7, organelles from the crude organellar pellet were resolved on a 15–45% Nycodenz (GIBCO BRL, Gaithersburg, MD) density gradient (McCammon et al., 1994). For Fig. 8, 50 μl from Nycodenz gradient fractions 1–4 were pooled and 800 μl of 50 mM Tris-Cl, pH 8.5, 10 mM DTT was added. The sample was incubated on ice for 1 h with intermittent vortexing. After this incubation, the extract was centrifuged at 128,000 *g* for 15 min in a Beckman TL-100 tabletop ultracentrifuge. The pellet was resuspended in the same buffer as the supernatant and both were precipitated with 10% TCA. The TCA precipitates were recovered and resolved by SDS-PAGE and immunoblotted.

Preparation of Metabolically Active Spheroplasts and CAT Trimerization Assay

Cells, cultured as above, were converted to spheroplasts in a similar fashion as above except that magnesium sulfate was used as the osmotic stabilizer. Washed, Tris-DTT-treated cells were resuspended and converted to spheroplasts in 0.55 M MgSO₄, 20 mM KPi, pH 7.5, 0.1% galactose using 2 μg/OD$_{600}$ U of Yeast Lytic Enzyme (ICN Biomedicals). The spheroplasts were harvested and resuspended at 10 OD$_{600}$ U/ml in semi-synthetic oleate medium containing 0.55 M MgSO₄ and 0.1% galactose. The spheroplasts were incubated for 2 h at 30°C to enhance subsequent radiolabeling. After this incubation, an aliquot of spheroplasts was removed and labeled with [³⁵S]methionine and cysteine (EXPRE³⁵S³⁵S; Amersham) at ~70 μCi/ml for 5 min at 30°C. Unlabeled methionine and cysteine were then added to 1 mM each and the spheroplasts were further incubated at 30°C or immediately processed. A 250-μl aliquot was removed and added directly to 750 μl of ice-cold 1.0 M SMA buffer, pelleted in a microfuge for 2 min at 4°C, and lysed in 200 μl of 10 mM Tris, pH 8.0, 5 mM EDTA, 50 mM sodium chloride, and 1% Triton X-100 (TENT). The lysate was cleared by centrifugation in a microfuge for 10 min at 4°C. After a 30 min chase at 30°C, another aliquot was removed, and processed as above. These cleared lysates were loaded onto a 4-ml 5–20% sucrose gradient containing TENT and centrifuged in a Beckman SW60 rotor for 15.5 h at 60,000 rpm (370,000 *g*$_{ave}$) and fractionated from the bottom. The fractions were prepared for immunoprecipitation by adding TENT to 1 ml final volume and 1 μl of anti–CAT antibody. Immune complexes were allowed to form on ice overnight. 10 μl Pansorbin (Calbiochem-Behring Corp., Palo Alto, CA) were then added on ice for 1 h and the immunoprecipitates were recovered by microcentrifugation. The samples were washed with TENT, resuspended in Laemmli sample buffer (Laemmli, 1970), and proteins were resolved by SDS-PAGE.

Plasmid Constructions

The HindIII-BamHI fragment of pCATC (Gould et al., 1988; gift of Suresh Subramani) containing the CAT-PMP20 coding region, was cloned into pDT-GCU (*GAL1-10, CEN4, URA3*) (Kang et al., 1990), creating pgC20p. Modifications of the COOH-terminus were performed by oligonucleotide-directed mutagenesis (Kunkel et al., 1987). The HindIII-BamHI fragment was cloned into M13 mpl9 and used as a template for mutagenesis. Sequences encoding the 12 amino acids from PMP20 were removed by looping out the corresponding 36 bp with the oligonucleotide C20-1 (see Table I). CAT-AKL was created by looping out the sequences corresponding to the nine amino acids before the AKL with the oligonucleotide C20-2. In the CAT-G9-AKL construct, the nine PMP20 amino acids prior to the AKL were replaced with nine glycine residues with the oligonucleotide C20-3. The mutations were confirmed by dideoxy sequencing (Sequenase; United

Table I. Oligonucleotides

Name	Sequence
C20-1	5'-CCCGGGGATCCTCTAGCCGGCCCCGCCCTCCCA-3'
C20-2	5'-CCTCTAGAGCTTCGCGCCGGCCCCGCCCTCCCA-3'
C20-3	5'-CCTCTAGAGCTTCGCGCCGCCGCCGCCGCCGCCGCCGCCGCCGGCCCCGCCCTCCCA-3'
C20-4	5'-CCTCTAGAGCTTGCAGCCGGCCCCGCCC-3'
C20-5	5'-CCTCTAGAGCTTCGAGCCGCCGCCGCCG-3'
CAT-NotI(+)	5'-GCTAAGGAAGCTAAAATGGGCGGCCGCGAGAAAAAAATCACTGG-3'

States Biochemical Corp., Cleveland, OH) and reconstructed in pgC20p to create the three new expression vectors pgC20-1C, pgC20-2B, and pgC20-3A encoding CAT, CAT-AKL, and CAT-G9-AKL, respectively. The AKL was changed to SKL as follows: single-stranded DNA containing the CAT-AKL construction was mutated to CAT-SKL with the oligonucleotide C20-4. Similarly, CAT-G9-AKL was mutated to CAT-G9-SKL with the oligonucleotide C20-5. These mutations were reconstructed in pgC20p to create the two new expression vectors pgC20-4E, and pgC20-5D, encoding CAT-SKL and CAT-G9-SKL respectively.

The yeast coexpression experiments used constructs that were based on the pRS310-314 plasmid series of Sikorski and Hieter (1989). pJM3A-GCH was created by the following manipulations: pgC20p was cut with AatII, filled in with Klenow, and cut with EagI. This fragment, which contained the GAL1-10 promoter, CAT-G9-AKL, and the phosphoglycerate kinase 3' terminator, was ligated into pRS313 (*CEN6, HIS3*) after digestion with EcoRV and EagI.

pJM1C-GCU was created by first inserting the GAL1-10 promoter into a modified pRS316 (*CEN6, URA3*), without the SalI, ClaI, HindIII, or EcoRV sites in the multiple cloning region, on an EcoRI-BamHI fragment. The remainder of the construct was generated by cutting pgC20-1C with HindIII and EagI. This fragment, which contained CAT and the phosphoglycerate kinase 3' terminator, was ligated into the pRS313 vector with the GAL1-10 promoter cut with HindIII-EagI.

Three copies of the hemagglutinin epitope tag (HA-tag) were fused to the amino terminus of CAT by first inserting a NotI site in CAT immediately 3' of the initiator methionine by oligonucleotide-directed mutagenesis. To accomplish this, a 250-bp EcoRI fragment containing the initiator methionine and the first 71 amino acids of CAT was cloned in M13mp19 (RI-CAT19). This construct was used to add an in-frame NotI site, generating the amino acids GGR. The oligonucleotide used for this manipulation was CAT-NotI(+). The resulting construct, RI-CAT19-NotI, was removed from M13mp19 by cutting with EcoRI and ligated into pUC18 cut with EcoRI giving pRICAT18-NotI. Three copies of the HA tag were removed from pSM491 (obtained from Carol Berkower and Susan Michaelis) by digesting with NotI. The resulting 109-bp fragment was ligated into pRICAT18-NotI, generating pRICAT18-HA. The EcoRI fragment was reconstructed back into pJM1C-GCU, generating pJM1CHA-GCU. All mutations were confirmed by sequencing.

Expression in animals cells required reconstruction of CAT-G9-AKL and HA-CAT into the animal cell expression vector pCMV5 (Andersson et al., 1989). Thus, pCMV5-3A was created by inserting CAT-G9-AKL into pCMV5 by cutting both pCMV5 and pJM3A-GCH with HindIII and BamHI. pCMV5-1C was created similarly by removing CAT from pJM1C-GCU on a HindIII-BamHI fragment and ligating the fragment into pCMV5 which had been cut with HindIII and BamHI. The HA tag was added, creating pCMV5-1CHA, by cutting pRICAT18-HA with HindIII-BspEI, which contains the NH$_2$-terminus of CAT with the HA tag, and ligating the fragment into pCMV5-1C. Transfection-quality DNA was obtained for animal cell transfection using the Qiagen Maxiprep kit according to the manufacturer's instructions.

SDS-PAGE and Immunoblotting

Standard 9% Laemmli gels (Laemmli, 1970) were used throughout. Unstained and pre-stained molecular weight markers were from Bio-Rad Laboratories (Cambridge, MA). Protein precipitations by TCA were done according to McCammon et al. (1994). Immunoblotting was performed as described by Towbin et al. (1979) using the enhanced chemiluminescence (ECL; Amersham Corp., Arlington Heights, IL) method of detection as recommended by the manufacturer. The anti-CAT polyclonal antibody, (5 Prime-3 Prime Inc., Denver, CO), was used at a dilution of 1:1,000 for im-

munoblotting. The anti-thiolase antibody, kindly provided by Jon Rothblatt (Dartmouth, Hanover, NH), was used at a dilution of 1:30,000 in combination with the anti-acyl CoA oxidase antibody (McNew et al., 1993) at a dilution of 1:500. The HA monoclonal antibody 12CA5 (BABCO; gift of Melanie Cobb, University of Texas Southwestern, Dallas, TX) was used at a dilution of 1:1,000. The anti-PMP24 antibody will be described elsewhere (Marshall, P., and J. M. Goodman, manuscript in preparation), and was used at a dilution of 1:1,000. The intensity of bands from films were quantitated by densitometry (Zenith Soft Laser Scanning Densitometer, Biomed Instr.).

Immunoelectron Microscopy

Approximately 100 OD$_{600}$ U of cells were centrifuged through 2% gelatin in 0.1 M sodium phosphate buffer, pH 7.4, and placed on ice for 10 min. 0.5–1.0-mm blocks of cells were cut from the gelatin pellet and placed in 0.5% glutaraldehyde, 2% paraformaldehyde in 0.1 M phosphate buffer on ice for 1 h. Blocks of cells were infused with 2.3 M sucrose in phosphate buffered saline containing 25% polyvinylpyrolidone (M_r 10,000) for 1 h at room temperature. Selected blocks were mounted on aluminum pins, frozen, and stored in liquid nitrogen. Cryosections 80–100-nm thick were cut on an ultramicrotome (Leica Inc., Deerfield, IL) at −80°C as described (Griffiths et al., 1984). For immunolabeling, the sections were collected on glow-discharged carbon-coated formvar films supported by 200-mesh hexagonal copper grids (Ted Pella, Inc., Redding, CA). Immunolabeling was carried out as described (Hartfield et al., 1991). The sections were incubated with the primary anti-CAT antibody diluted 1:1 with 5% fetal calf serum (GIBCO BRL, Gaithersburg, MD) in phosphate-buffered saline containing 0.12% glycine for 45 min at room temperature. Protein A, conjugated to 10 nm gold from a stock of 0.2 OD$_{520}$, was used at a dilution of 1:50 in 5% fetal calf serum in phosphate buffered saline containing 0.12% glycine for 30 min at room temperature. Sections were imaged on Kodak SO163 film using a Jeol 1200 electron microscope operating at 80 kV.

Animal Cell Transfection and Immunofluorescence Microscopy

CV-1 cells were seeded at ∼70% confluency in DME containing 10% fetal calf serum and antibiotics (50 U/ml penicillin G and 50 μg/ml streptomycin) and grown for 24 h. The cells were washed in DME and transfected using Lipofectin (GIBCO BRL) according to the manufacturer's instructions. Cells were transfected with pCMV5-3A or pCMV5-1CHA individually or in combination for 6 h. Then the lipofectin-DNA containing media was removed and replaced with fresh DME with 10% FCS and antibodies. At 48-h posttransfection, the cells were split, plated on coverslips and grown overnight. The transfected cells were processed for double indirect immunofluorescence 64 h after transfection as follows: cells were washed two times with PBS, and then fixed with 4% paraformaldehyde (Fluka Chemic AG, Buchs, Switzerland) in PBS for 20 min at room temperature. The paraformaldehyde fixation was quenched by a wash with DME. The cells were then washed once with PBS, and then twice with PBS + 1% BSA. Next, the cells were permeabilized by incubating in PBS + 1% BSA + 0.1% Triton X-100 for 15 min at room temperature. They were then washed once with PBS and twice with PBS-1% BSA. Primary antibody (anti-CAT or -HA IgG derived from monoclonal antibody 12CA5, Boehringer-Mannheim Biochemicals, Indianapolis, IN) in PBS-1% BSA was then added as described in the legend for Fig. 9. Cells were incubated with primary antibody for 30 min. They were then washed as before and fluorescent secondary antibodies were added. Both second antibodies (Fisher Scientific, Pittsburgh, PA), goat anti-rabbit IgG conjugated to Texas red and goat anti-mouse IgG conjugated to FITC, were used at 1:100 (1 μg/ml). Finally, the cells were washed

twice with PBS-1% BSA, twice with PBS, and then mounted on slides. The slides were viewed on a Zeiss confocal microscope and photographs were taken on Kodak Tmax 100 film.

Results

PTS1 Is Sufficient for Peroxisomal Import in Saccharomyces cerevisiae

We have developed a system for examining the sorting of heterologous proteins to the peroxisome in *Saccharomyces cerevisiae* in vivo (McCammon et al., 1994). The heterologous protein is expressed on a centromeric plasmid driven by the inducible *GAL1-10* promoter. Cells are grown with oleic acid as the sole carbon source to induce the proliferation of peroxisomes, and expression of the heterologous protein is accomplished by the addition of galactose. We use low levels (0.1–0.2%) of galactose to limit the negative effects of this carbon source on peroxisomal proliferation (McCammon et al., 1990) as well as to maintain relatively low levels of expression to avoid aberrant sorting. After peroxisomal induction and plasmid expression, the cells are converted to spheroplasts, osmotically lysed, and organelles are fractionated, first into a 25,000 g crude organellar pellet (containing mainly peroxisomes and mitochondria) and supernatant. Mitochondria and peroxisomes can then be separated on sucrose or Nycodenz gradients.

Using these techniques, we tested the ability of peroxisomal targeting sequences to drive the import of chloramphenicol acetyltransferase, a homotrimeric bacterial protein encoded by the Tn9 transposon (Shaw and Leslie, 1991). CAT has a subunit molecular mass of 25,700 D. We first tested a protein fusion termed CAT-PMP20 that sorts with high efficiency to animal peroxisomes (Gould et al., 1990a). This hybrid consisted of CAT followed by the final 12 amino acids of the peripheral membrane protein PMP20 (DVS-TAQKIIAKL; see Table II) from *Candida boidinii*. Unmodified CAT was used as a negative control.

Fig. 1 illustrates the partitioning of these proteins, and others described below, between crude organellar pellet (P) and supernatant (S) fractions. It also shows the partitioning of two peroxisomal matrix proteins, acyl CoA oxidase (ACO), and 3-ketoacyl CoA thiolase, as controls for fractionation. As we have found before, thiolase tended to leak more readily from peroxisomes than acyl CoA oxidase (McCammon et al., 1990). It is clear from the figure that most of CAT-PMP20 (81% in this experiment) partitioned to the pellet, suggesting that it correctly sorted to peroxisomes. In other experiments, a greater percentage was detected in the supernatant. This was mirrored, however, by greater leakage of thiolase (data not shown). In contrast, all of unmodified CAT remained in the supernatant.

To confirm that CAT-PMP20 had associated with peroxisomes, the organellar fraction from a similar experiment was subjected to sedimentation through a sucrose density gradient (Fig. 2). Fig. 2 A illustrates the protein profile from a typical gradient. Peroxisomes sediment to fractions 4 and 5 in this system (Fig. 2 B) while mitochondria remain in the top half of the gradient. A significant but variable amount of catalase also appears at the top of the gradient in fraction 1 due to leakage from some peroxisomes and contamination of unbroken oleate-filled spheroplasts (McCammon et al., 1990). It is clear that the migration of CAT-PMP20 in this

Table II.

CAT-PTS1 Constructs*

CAT-PMP20		
−EGGA	V	**DVSTAQKI IAKL**
CAT		
−EGGA	G	
CAT-AKL		
−EGGA	G	**AKL**
CAT-G9-AKL		
−EGGA		**GGGGGGGGGAKL**
CAT-SKL		
−EGGA	G	**SKL**
CAT-G9-SKL		
−EGGA		**GGGGGGGGGSKL**

* Plain text shows the last four amino acids of CAT; bold text illustrates the amino acid created during the construction; and bold italic text describes the additions at the extreme carboxy terminus.

gradient closely followed the marker enzyme catalase, confirming that the construct sorted to peroxisomes. Thus, the COOH-terminal 12 amino acids of PMP20 were sufficient for sorting in *S. cerevisiae*. CAT enzymatic activity was observed in fraction 5 from this gradient (data not shown), indicating that at least some of the protein was properly assembled into a trimer. No unmodified CAT appeared in a parallel gradient since it was all cytosolic.

Next, constructs were made to test the contribution of the nine amino acids (DVSTAQKII) preceding the carboxy-terminal AKL of PMP20 (Table II). Nine glycines were substituted for this sequence (in the construct CAT-G9-AKL), or the sequence was deleted entirely (CAT-AKL) to determine whether AKL was sufficient for targeting. Data in Figs. 1
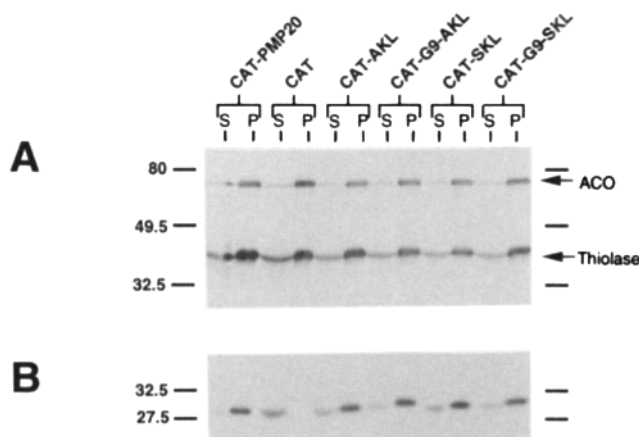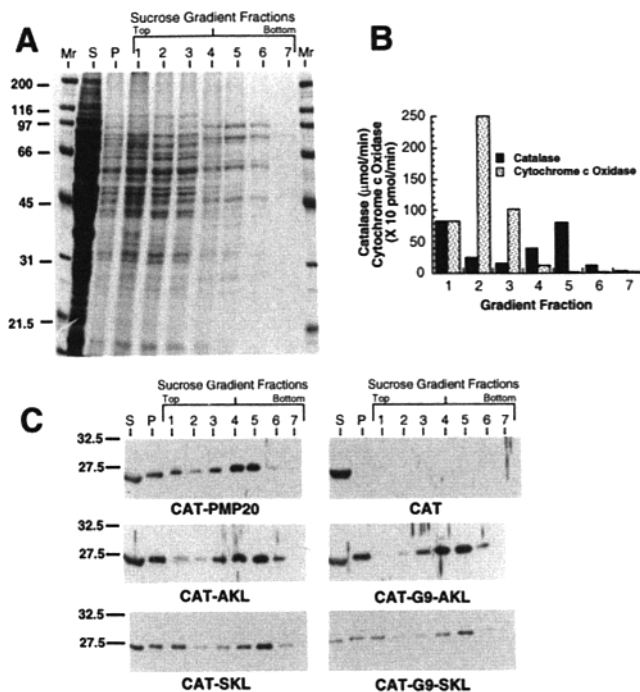

Figure 1. CAT-PTS1 chimeras fractionate to a particulate fraction. Induced cells expressing the indicated CAT constructs were fractionated into 25,000 g supernatants and pellets. An equal percentage of each supernatant (S) and pellet (P) was resolved by SDS-PAGE, transferred to nitrocellulose and immunoblotted with various antibodies as follows. (A) Immunoblot using antibodies against the peroxisomal marker proteins thiolase and acyl CoA oxidase (ACO) in combination. (B) Immunoblot using anti-CAT antibody. The secondary antibody in all cases was a donkey anti–rabbit IgG at a dilution of 1:5,000. Positions and masses (in kD) of molecular weight markers are indicated.

Figure 2. CAT-PTS1 chimeras sort to peroxisomes. 25,000 g pellets were fractionated on discontinuous sucrose gradients. (S and P) Supernatant and pellet from the 25,000 g centrifugation. (A) A representative Coomassie-stained gel illustrating the pattern of total proteins obtained by this method. (B) The gradient seen in A was analyzed for the marker enzymes catalase (peroxisomes) and cytochrome c oxidase (mitochondria). Values are total activities from the fractions. (C) Immunoblots of the CAT constructs, expressed separately, using the anti-CAT antibody. Molecular weight markers, in kD, are indicated to the left of A and C.

Figure 3. CAT-G9-AKL is imported into the peroxisome. Frozen thin sections from cells expressing CAT-G9-AKL were incubated with the anti-CAT antibody and processed for immunogold electron microscopy. Bar, 200 nm.
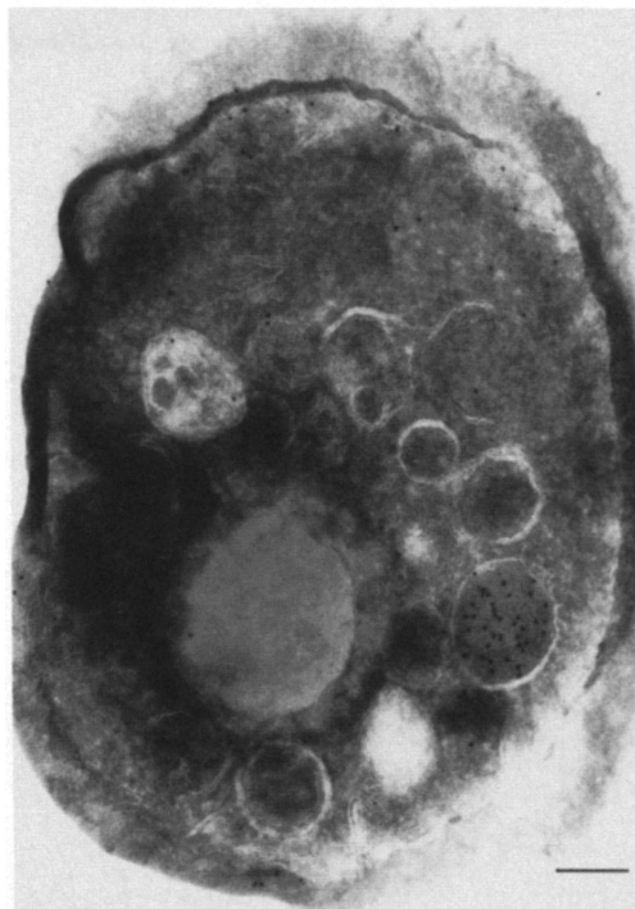
and 2 indicated that both proteins sorted to peroxisomes to about the same extent as CAT-PMP20. Thus, AKL is sufficient for this process, at least in the context of CAT. Finally, constructs containing G9-SKL or SKL alone were tested, since SKL was found not to sort when placed behind DHFR (Distel et al., 1992). These proteins sorted to peroxisomes as well. Based on the results from several experiments we found that the G9 spacer usually had a positive effect on sorting, and AKL constructs were more efficient for sorting than the corresponding SKL constructs.

To confirm that the CAT-PTS1 constructs were imported into peroxisomes and not simply bound to the outside surface of the organelle, cells expressing CAT-G9-AKL were subjected to immunoelectron microscopy. The results, shown in Fig. 3, clearly indicate that this molecule is localized to the organelle and is distributed randomly within the matrix. Unmodified CAT did not localize to peroxisomes (data not shown).

Thus, PTS1 tripeptides can target CAT to peroxisomes in S. cerevisiae, as they can to animal peroxisomes and trypanosomal glycosomes (Gould et al., 1989; Blattner et al., 1992).
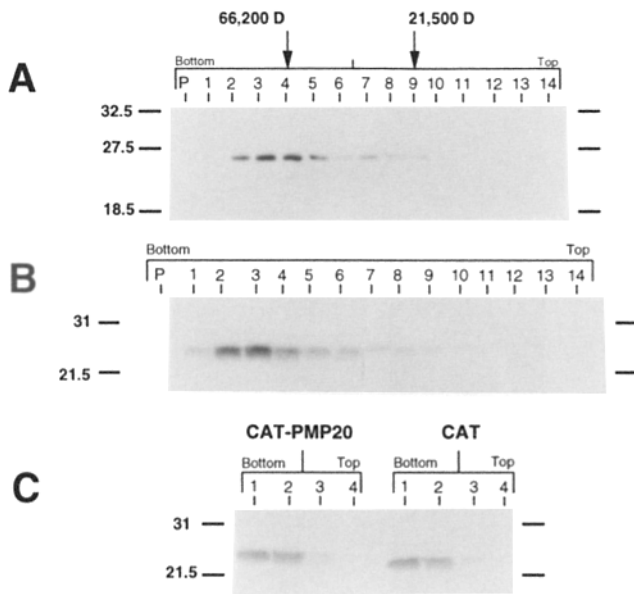
CAT Trimerizes Rapidly in S. cerevisiae

Preliminary experiments suggested that import of CAT-PTS1 proteins occurred over many hours. Using our standard cul-

turing conditions, the cellular concentration of CAT reached a plateau 8 h after the addition of galactose while the fraction of CAT found in organellar pellets compared to supernatants appeared to increase over several more hours (data not shown). Difficulties in controlling for similar protein recoveries in organellar fractions at each time point, however, made the analysis difficult.

These results prompted us to analyze the rate of CAT trimerization. Since CAT-PTS1 constructs were competent for import, we assumed that the active species for import was the monomer, and we predicted that the rate of trimerization would be at least as slow as the rate of import in yeast. To determine the rate of CAT trimerization in vivo, cells expressing CAT were cultured as usual, converted to spheroplasts and metabolically radiolabeled with [35S]methionine and cysteine for 5 min. Excess unlabeled methionine and cysteine were added and the cells were either lysed immediately in detergent-containing buffer on ice or further incubated for 30 min at 30°C and then lysed. Lysates were subjected to centrifugation through sucrose velocity gradients under conditions where trimers migrate into the bottom half of the gradient while monomers should remain in the top half. Fig. 4 A shows the migration of mature CAT in this gradient system. Surprisingly, all of the CAT was found to be
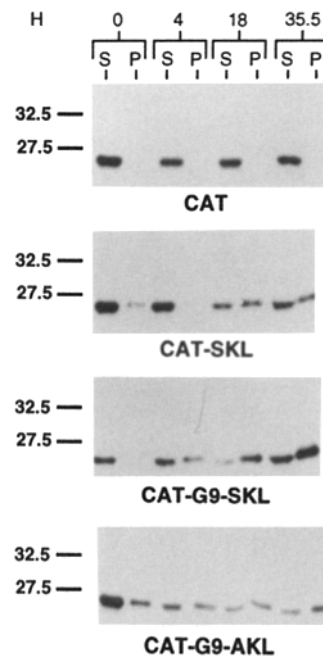
Figure 4. CAT trimerizes very rapidly in S. cerevisiae. (A) The 25,000 g supernatant from cells expressing the unmodified CAT construct was concentrated by Amicon ∼10-fold. 200 μg of BSA (66,200 D) and 200 μg STI(21,500 D) were added to 200 μl of the concentrated supernatant and centrifuged through a 4-ml 5–20% continuous sucrose gradient. Proteins in fractions were resolved by SDS-PAGE and immunoblotted with the anti-CAT antibody. The positions of BSA and STI in the gradients, determined by staining with Coomassie, are indicated. (B) Induced cells were converted to metabolically active spheroplasts and radiolabeled for 5 min at 30°C. Excess unlabeled methionine and cysteine were added and the cells were lysed immediately in detergent-containing buffer. The lysate was centrifuged through a 5–20% sucrose gradient as above and fractionated. Gradient fractions were immunoprecipitated with the anti-CAT antibody and analyzed by SDS-PAGE and autoradiography. (C) Cells expressing either CAT-PMP20 or unmodified CAT were radiolabeled for 5 min and immediately analyzed as above (B) except that the gradients were fractionated into four fractions instead of 14. (P) Pellets from the sucrose gradients, which were resuspended in a volume of TENT equal to the other fractions were processed identically.

Figure 5. CAT-PTS1 proteins are imported over hours. Cells expressing the indicated CAT-PTS1 constructs were precultured as normal except that galactose was added 8 h prior to the change to semi-synthetic oleate medium. Cells were harvested at 0, 4, 18, and 35.5 h after the change to semi-synthetic oleate medium, converted to spheroplasts, and fractionated into 25,000 g supernatants (S) and pellets (P) as usual. Equal percentages of S and P were resolved by SDS-PAGE and immunoblotted with the anti-CAT antibody.

trimeric by the end of the 5-min pulse (Fig. 4 B). In contrast, these lysis conditions prevented the oligomerization of newly synthesized alcohol oxidase, a peroxisomal protein of methylotrophic yeasts (Goodman et al., 1984). The migration pattern was identical when cells were incubated for an additional 30 min with excess unlabeled amino acid (data not shown). This fast rate of trimerization was not unique to unmodified CAT. Modification of the carboxy terminus with PTS1, the last 12 amino acids of PMP20, yielded identical results (Fig. 4 C). While we cannot formally rule out that some trimerization occurred during lysis, this should be minimal due to the massive dilution of the cytoplasm upon cold lysis. Thus, trimerization of CAT appears to occur in vivo within a few minutes.

CAT Is Imported as a Trimer

The kinetics of CAT trimerization in vivo suggested that CAT trimers containing PTS1 may be imported into the peroxisomal matrix. To confirm this idea, we expressed 3 CAT-

PTS1 constructs in the absence of induced peroxisomes to determine whether preformed trimers could be imported once peroxisomal proliferation was allowed to proceed. For this experiment cells were first cultured in 0.2% galactose for 8 h to induce the expression of CAT constructs, then galactose was removed and the cells were transferred to oleic acid to induce peroxisomal proliferation. At different times after the addition of oleic acid, cells were converted to spheroplasts and crude organellar pellets and supernatants were obtained (Fig. 5). The unmodified CAT control was always found in the supernatant since it did not contain a PTS. Only a minor fraction of the CAT-PTS1 proteins pelleted at t_0 (immediately after transfer to oleic acid), indicating that most of the molecules were still in the cytosol and had not yet associated with peroxisomes. This was confirmed by a subsequent centrifugation of the medium-speed supernatant at 100,000 g, indicating that the proteins were not in a small organelle (data not shown). Over several hours, however, much of the preexisting soluble CAT-PTS1 proteins disappeared from the cytosol fraction and appeared in the pellet fraction. The fraction of fusion protein in the pellet at $t_{35.5}$ varied from 35% for CAT-SKL to 75% for CAT-G9-AKL. Some variability in recovery of total CAT-PTS1 protein between time points was seen due to different efficiencies of spheroplasting and spheroplast lysis during the course of the experiment. No CAT was detectable if galactose was not added to the culture medium (data not shown).

These data support the hypothesis that preformed CAT trimers were capable of peroxisomal import. Although trimeric CAT is very resistant to subunit dissociation and denaturation in vitro (Shaw and Leslie, 1991), it is possible that the trimers had undergone dissociation into monomers before being imported. To rule out this possibility, we co-expressed CAT-G9-AKL with CAT containing three copies of an epitope tag from influenza virus hemagglutinin but no PTS1 (HA-CAT). If only unfolded monomeric subunits are competent for import, then HA-CAT should never associate
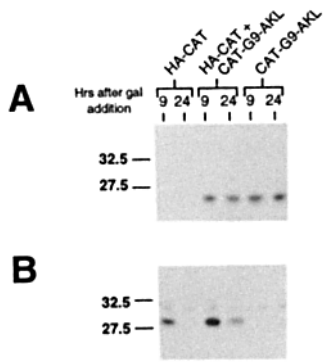
Figure 6. HA-CAT is less stable than CAT-G9-AKL and is not recognized by the anti-CAT antibody. Cells expressing HA-CAT alone, both HA-CAT and CAT-G9-AKL, or CAT-G9-AKL alone were cultured as normal. At 9 and 24 h after the addition of galactose, cells were removed, and broken with glass beads to yield whole-cell lysates. Proteins were resolved by SDS-PAGE and immunoblotted with either the anti-CAT antibody (*A*) or the anti–HA monoclonal antibody 12CA5 (*B*). The upper band in (*B*) is a cross-reacting host protein.

with this organelle. Conversely, if trimers can cross the peroxisomal membrane, then CAT-G9-AKL should be capable of transporting HA-CAT into the peroxisome as a heterotrimer.

There were two unexpected observations that were seen upon expressing HA-CAT in yeast, and these are illustrated in Fig. 6. First, the HA-tagged protein was not detectable with the anti-CAT antibody. This suggested that the unmodified extreme amino terminus of CAT was critical to the recognition of this protein by the anti-CAT antibodies. The lack of recognition made it difficult to compare the relative concentrations of the two proteins. The second observation was that HA-CAT, or at least the HA epitope, was considerably less stable than the CAT-PTS1 fusion proteins. The half-lives of CAT-PTS1 fusions were greater than 40 h in yeast (data not shown). In contrast, when HA-CAT was expressed alone and cells were harvested at the normal time (24 h after galactose addition), no HA-CAT was detectable, although the protein was clearly seen after only 9 h. Significantly, the degradation of HA-CAT was slowed by the co-expression of CAT-G9-AKL. Thus, at 9 h following addition of galactose, there was twice the amount of detectable HA-CAT in cells expressing both constructs compared with those expressing only HA-CAT. After 24 h HA-CAT was seen (19% remained compared to the 9-h time point) only when both were expressed. Perhaps HA-CAT homotrimers dissociate more readily than CAT or CAT-PTS1 homotrimers, yielding an unstable monomeric species. Regardless, our result suggested that heterotrimers were formed, and that this species protected HA-CAT from degradation.

Because the HA-CAT was relatively unstable, cells were harvested at an earlier time point (15 h after galactose addition instead of 24 h) to determine its intracellular localization. Organelles were purified on a Nycodenz gradient instead of sucrose. Under normal culturing conditions (harvesting 24 h after galactose), mitochondria and peroxisomes migrate to opposite ends of this gradient with essentially no overlap (McCammon et al., 1994). At 15 h, a distinctive pattern of total proteins in this gradient can still be seen, such that peroxisomes peak in fractions 2 and 3 while the mitochondria peak in fractions 9 and 10 (Fig. 7 *A*). At this earlier time point, however, we reproducibly saw that both organelles migrate more diffusely in the gradient.

When HA-CAT was expressed alone, no immunoreactivity
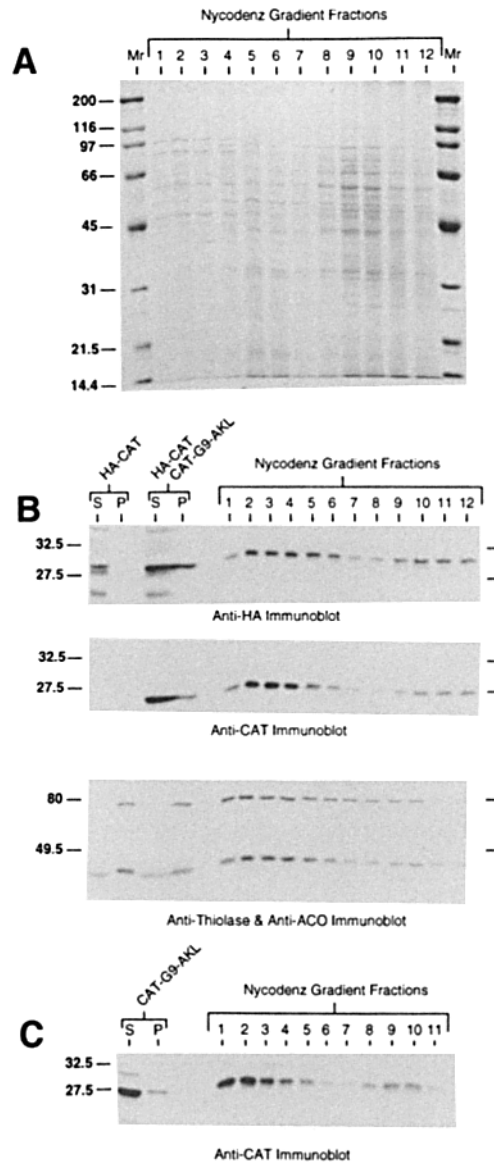
Figure 7. HA-CAT co-fractionates with peroxisomes. Cells expressing HA-CAT, CAT-G9-AKL, or both were precultured as normal. At 15 h after the addition of galactose, cells were harvested and 25,000 *g* supernatants and pellets were prepared. The 25,000 *g* pellet from cells expressing CAT-G9-AKL or both constructs were further fractionated on 15–45% Nycodenz gradients. The gradients were fractionated from the bottom. (*A*) The gradient fractions from cells expressing both constructs were resolved by SDS-PAGE and stained with Coomassie. (*B*) Fractions from the gradient described in *A* (expressing both constructs in combination) were subjected to SDS-PAGE, transferred to nitrocellulose, and immunoblotted with the anti-HA antibody, the anti-CAT antibody, or with anti-ACO and anti-thiolase in combination. Additionally, the 25,000 *g* supernatant and pellet from cells expressing only HA-CAT were also included (left two lanes). (*C*) Gradient fractions from cells expressing only the CAT-G9-AKL construct were immunoblotted with the anti-CAT antibody. The presence of Nycodenz in the gradient fractions caused minor differences in electrophoresis resulting in the uneven pattern seen.

was found in the organellar pellet as expected, since this protein lacks a PTS (Fig. 7 B, first two lanes). When both proteins were expressed, however, 32% of the detectable HA-CAT was in the organellar pellet. A few minor host soluble proteins can be seen that cross-reacted with the HA antibodies. Another yeast cytosolic protein of 90 kD that stained intensely with the HA antibody is not shown. Most of the pelletable HA-CAT migrated with CAT-G9-AKL and the peroxisomal markers thiolase and acyl CoA oxidase in the gradient, indicating that HA-CAT had indeed associated with peroxisomes. CAT-G9-AKL behaved similarly when it was expressed alone (Fig. 7 C). It should be noted that at this earlier time point some peroxisomal protein, both markers and CAT constructs, localized at the top half of this isopycnic gradient, where only mitochondria are normally found (McCammon et al., 1994). The possible significance of this observation is discussed below.

It is imaginable that HA-CAT, when expressed with CAT-G9-AKL, is tightly aggregated onto the outside surface of peroxisomes or trapped within the membrane, rather than existing inside the organelle. The nonspecific cross-reactivity of the anti-HA-antibody to other yeast proteins obviated the cytochemical experiment to test this possibility. Instead, we exploited the finding that yeast peroxisomes release matrix proteins at slightly alkaline pH (8.0–8.5) compared to pH 5.5 or 6.0 (Goodman et al., 1984). If HA-CAT is aggregated on the outside surface of peroxisomes or stuck in the membrane, it should not be released by pH 8.5 and mild ionic strength since it survived the conditions of centrifugation. When purified peroxisomes from the Nycodenz gradient were exposed to this treatment, all of CAT-G9-AKL was released, as well as 86% of HA-CAT (Fig. 8). We believe that the remaining 14% of HA-CAT has dissociated from trimers (consistent with its instability) and has aggregated to other proteins or to the membrane. Almost all of thiolase (94%) was released, whereas only half of acyl CoA oxidase, a matrix enzyme which is normally more tightly associated to the organelles (McCammon et al., 1990) was released. In contrast, the integral membrane protein PMP24 was not extracted after this treatment. This experiment confirms that HA-CAT is being imported into the matrix compartment when co-expressed with CAT-G9-AKL.
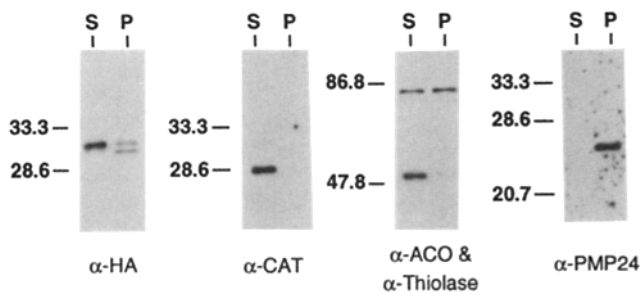
Figure 8. HA-CAT is extracted with matrix proteins. Nycodenz gradient-purified peroxisomes were extracted with 5 vol of 50 mM Tris-Cl, pH 8.5, containing 10 mM DTT for 1 h on ice with intermittent vortexing. This extract was centrifuged at 128,000 g for 15 min to yield a supernant (S) and pellet (P), which were precipitated with TCA, resolved by SDS-PAGE, and transferred to nitrocellulose. These samples were immunoblotted with antibodies to CAT, HA, thiolase, acyl CoA oxidase, and PMP24.

Oligomeric Import Is Not Restricted to Yeast

To test whether the import of CAT trimers could occur in animal cells, we examined the localization of CAT-G9-AKL and HA-CAT after transient transfection of monkey CV-1 cells. When CAT-G9-AKL was expressed alone, it localized, as expected, to discrete, punctate structures characteristic of peroxisomes in this organism (Fig. 9 A, Gould et al., 1987, 1990b). In contrast, a diffuse cytoplasmic staining was observed after the transfection of HA-CAT alone (Fig. 9 B). When these two proteins were co-expressed, both yielded a punctate pattern with variable levels of cytoplasmic staining (Figure 9, C–F). This observation indicated that HA-CAT can sort to the peroxisome in CV-1 cells when it is co-expressed with CAT-G9-AKL.

Discussion

In this report we have shown that a PTS1 tripeptide is sufficient for peroxisomal targeting in S. cerevisiae, and that CAT containing a PTS1 sequence is imported as an oligomer into yeast and animal cell peroxisomes in vivo.

Many proteins of the microbody matrix contain SKL, or a closely related variant, at their extreme carboxy termini. These include proteins of peroxisomes, glyoxysomes, and glycosomes (Keller et al., 1991). It has been shown in many systems that the PTS1 tripeptide is necessary for targeting. However, only in the CV-1 system and in trypanosomes has it been shown that the tripeptide, fused to CAT, is sufficient for targeting (Gould et al., 1989; Blattner, et al., 1992). We now show that it is also sufficient in yeast. It should be noted that the same carrier protein, CAT, has been used in all cases. While we show here that AKL or SKL, fused to CAT, is sufficient for sorting in S. cerevisiae, Aitchison et al. reported that CAT-AKI did not localize to peroxisomes in this organism (Aitchison et al., 1991), although this sequence was necessary for peroxisomal import in an unrelated yeast, Candida tropicalis.

Import of our CAT proteins is slow relative to the import of endogenous proteins. Kinetics of import of endogenous matrix proteins have only been studied in a few cases, and this process generally occurs over several minutes. In rat liver, 50% of catalase is imported over 14–15 min while urate oxidase is almost entirely peroxisomal by the end of a 4-min labeling (Lazarow and de Duve, 1973; Lazarow et al., 1982). In Candida boidinii, half of alcohol oxidase, dihydroxyacetone synthase, and the peripheral protein PMP20 are imported over 20, 7, and 5 min, respectively (Goodman et al., 1984, 1992).

Our CAT constructs are imported over several hours. An objection can be raised that the slow kinetics that we observe may indicate that the import of oligomers is nonphysiological and reflects an aberrant process that is never seen with normal peroxisomal proteins. While only future experiments with native proteins will conclusively answer this question, the fact that oligomeric import occurs in animals (Fig. 9) as well as yeast increases the likelihood that this process is physiological and not simply an abnormality in yeast. There is also a precedent for the slow import kinetics of a native protein. In contrast to the rapid kinetics of catalase import in intact liver, import in human fibroblasts occurs over two hours or more. Moreover, tetramerization of catalase monomers in the cytoplasm, creating an active enzyme, precedes
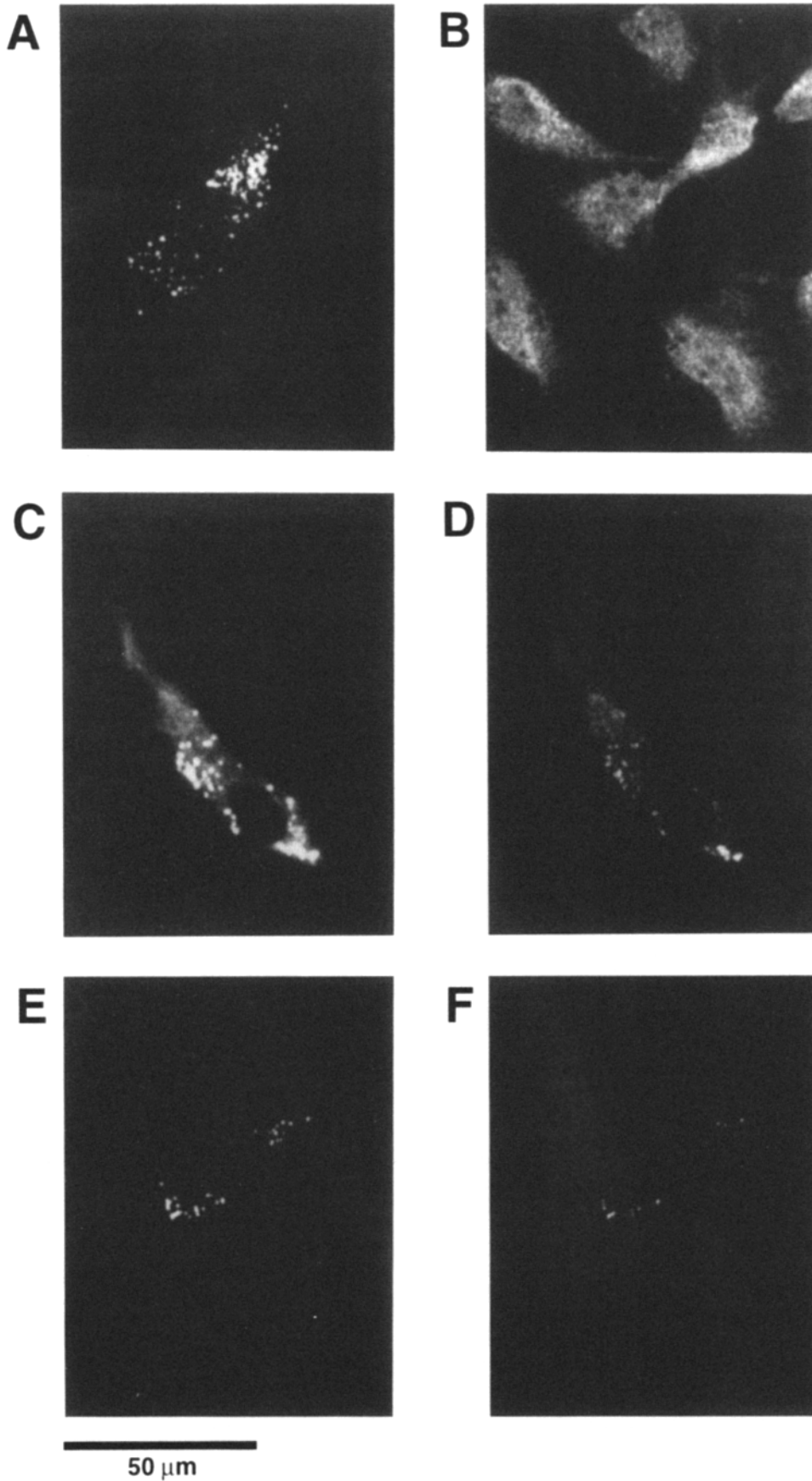
Figure 9. HA-CAT co-localizes with CAT-G9-AKL when co-expressed in animal cells. CV-1 cells were transfected with CAT-G9-AKL (*A*), HA-CAT (*B*), or both in combination (*C–F*). The cells were processed for double indirect immunofluorescence 64-h posttransfection and viewed on a Zeiss confocal microscope. (*A*, *C*, and *E*) CAT-G9-AKL immunolocalized with the CAT antibody (1:100 in *A*, 1:200 in *C* and *E*) and goat anti–rabbit IgG conjugated to Texas red. (*B*, *D*, and *F*) HA-CAT immunolocalized with the 12CA5 HA monoclonal antibody (1:50 in *B*, 1:20 in *D*, 1:100 in *F*) and goat anti–mouse IgG conjugated to FITC.

import into peroxisomes. Monomers and/or dimers are never seen without perturbing the system with drugs (Middelkoop et al., 1993).

It can be argued that the rate of CAT import is particularly slow because it is an oligomer, and that unfolded monomers may be imported much faster. This may be true. However, there is no previous data to indicate that peroxisomal proteins containing a PTS1 are imported as unfolded monomeric proteins. The kinetics of oligomerization vs. import has been studied in two cases: catalase in rat liver (Lazarow and de Duve, 1973), and alcohol oxidase in *C. boidinii* (Goodman et al., 1984). In both cases the kinetics of oligomerization were close to that of organellar association. The simplest interpretation of these data based on the mechanism of import into other organelles is that import precedes oligomer formation. However, it is possible that an oligomer is at least as efficient as a monomer for import. Furthermore, neither of these proteins contain a PTS1 motif.

It is reasonable to assume that the import of an artificial protein may be slower than a native protein. Unfortunately, there are no published data that systematically compare the rate of sorting of a carrier protein containing only the tripeptide signal compared to constructs with more extensive carboxy termini derived from peroxisomal sequences. The last 12 amino acids of PMP20 linked to CAT, for example, is a stronger targeting signal than simply AKL in the CV-1 system (S. Subramani, personal communication) and has been repeatedly used as a marker for peroxisomes in this system. Sequences in addition to PTS1 may confer secondary or tertiary structure which could increase the efficiency of targeting.

Another major factor that probably contributes to the slow sorting kinetics of the CAT proteins in our system is the presence of galactose during their expression. Galactose represses peroxisomal proliferation in yeast (Trumbly, 1992); it is converted to glucose, a classical repressor. We have had difficulty in the past purifying intact peroxisomes after galactose treatment. We believe that galactose may cause inactivation of peroxisomal import. This may explain why most of the import of the CAT proteins is primarily occurring after galactose is removed or used up, and cells regain peroxisomal function as they resume oleic acid utilization. This predicts that import will be faster if the galactose promoter is avoided in future constructs.

In fact, if organelles are prepared at an intermediate time (15 h) after the addition of galactose, a significant amount of peroxisomal protein, both marker and newly synthesized CAT-PTS1, is seen at a position of the Nycodenz gradient of a lighter density (see Fig. 7). While this could represent a normal subpopulation of lighter peroxisomes in which import occurs (Heinemann and Just, 1992; Luers et al., 1993), it may also be a response to galactose, in which a wave of budding of immature organelles follows the disappearance of the repressive carbon source.

Not all matrix proteins contain PTS1 or PTS2 sequences. Notable exceptions are yeast acyl CoA oxidase and catalase (Cohen et al., 1988; Hiltunen et al., 1992). There is data to suggest that both of these proteins require internal regions for import (Small et al., 1988; Kragler et al., 1993). An alternative explanation is that such proteins do not contain PTSs, but form import complexes with other proteins which do contain PTSs. For example, perhaps acyl CoA oxidase is

imported with the next enzyme in the fatty acid β-oxidation pathway, the multifunctional enzyme, which terminates in SKL. An association of these two proteins within the matrix has been seen in that they are released together from the organelle following treatment with high pH (J. M. Goodman, unpublished results). An import complex of alcohol oxidase and dihydroxyacetone synthase has also been observed in *C. boidinii* (Bellion and Goodman, 1987).

There has been previous data to suggest that oligomeric proteins can be imported into peroxisomes. The first such case involved the fusion of two different complementation groups of Zellweger fibroblasts (Brul et al., 1988). When these cells were fused, peroxisomal assembly was recovered, and tetrameric catalase from the cytosol was imported into peroxisomes. Pre-existing catalase was shown to be the active species since the process was unaffected by the addition of cycloheximide. The import of tetrameric catalase also might have been seen in a more recent work involving yeast cells that had a temperature sensitive mutation in peroxisomal assembly (Waterham et al., 1993). After incubation at the nonpermissive temperature in which catalase was mainly cytosolic, a shift to the permissive temperature increased the amount of particulate catalase, suggesting that cytosolic catalase was imported into peroxisomes. Although this was interpreted by the authors as the import of newly synthesized catalase, it is reasonable that at least some of the import utilized pre-existing cytosolic catalase. More recently, Middelkoop et al. examined catalase assembly in normal human fibroblasts to try to address the earlier finding that active cytosolic catalase was found in Zellweger fibroblasts (Middelkoop et al., 1993). This group used conformation-specific antibodies to show that catalase formed tetramers within one hour of synthesis while it remains in the cytosol. It subsequently localizes to a particulate organelle, presumably the peroxisome, over several hours. They also found that the addition of aminotriazole slowed the accumulation of particulate catalase. The authors speculated that aminotriazole inhibited the dissociation of tetramer. It is equally plausible to us that aminotriazole inhibited oligomer formation and therefore import, since an increase in catalase monomers and dimers was detected after drug treatment. Human catalase has been shown to sort to the peroxisomes of *S. cerevisiae* and forms an active enzyme (de Hoop et al., 1993); the kinetics of tetramerization and import, however, has not been studied in this heterologous system.

Another example of import of oligomers was shown by Walton et al. (1992), who microinjected octameric alcohol oxidase into cells. Most of the injected material was found later in a particulate pattern by immunofluorescence. Many of the particles were peroxisomes as determined by marker analysis.

The pathway that we report in this paper resembles nuclear import more than translocation into mitochondria, endoplasmic reticulum, or export from bacterial cytoplasm. The diameter of the CAT trimer (the type III isozyme, the only CAT molecule whose three-dimensional structure has been determined) is roughly 60 Å (Leslie, 1990), much larger than a diameter that is required to accommodate an unfolded protein being "threaded" through the membrane. Yet clearly, there are no structures on the peroxisomal surface that are reminiscent of nuclear pores. However, freeze-fracture micrographs of yeast peroxisomes show small inter-

membranous particles although they are seen less frequently than in other organelles (de Duve, 1983). These particles are much smaller than nuclear pores but they may be large enough to permit the passage of a molecule the size of trimeric CAT (Fig. 10, *Static Pores*). Alternatively, hypothetical pores may be dynamic, similar to those envisioned by Dobberstein and Blobel for translocation across the endoplasmic reticulum (Blobel and Dobberstein, 1975). Thus, a protein destined for secretion, in association with the ribosome, was hypothesized to engage subunits in the membrane to form a pore. Once translocation of the molecule across the

Dynamic Pores   Static Pores   Membrane Internalization
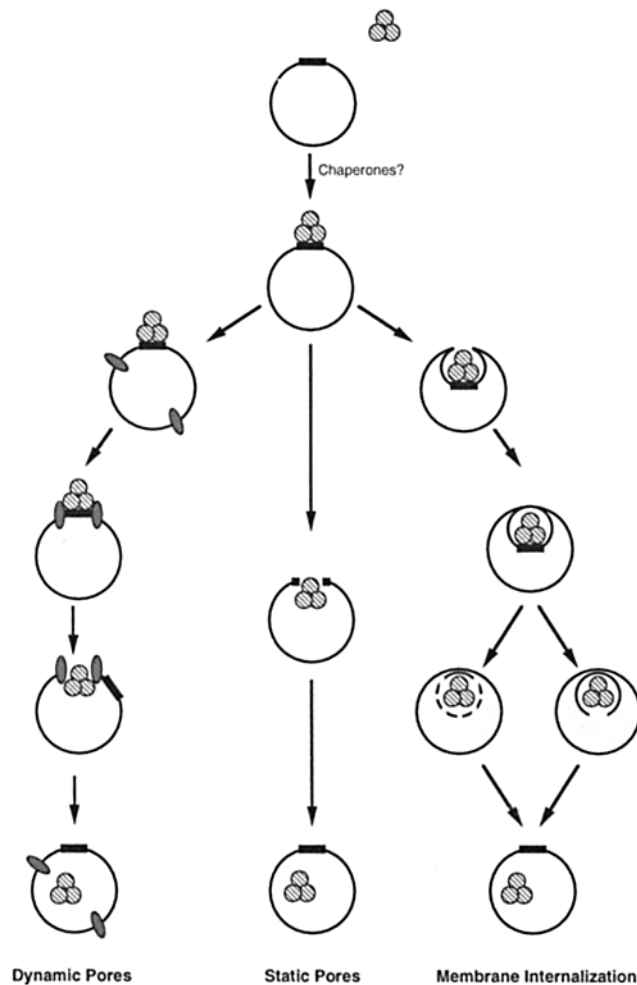
Figure 10. Possible mechanisms for trimeric CAT import. This figure illustrates three potential mechanisms of oligomeric protein import into the peroxisome. All models contain a membrane binding site (*solid rectangle*), presumably a proteinaceous receptor that binds to an oligomer (*three hatched circles*). The role of molecular chaperones in this process remains undetermined. The static pore model (*middle*) predicts that the membrane receptor is the pore. The dynamic pore model (*left*) predicts that pore components (*stippled ovals*) are recruited after membrane binding occurs which form a pore through which the oligomer passes. After import, the subunits dissociate. The membrane internalization model (*right*) predicts that membrane binding of an oligomer induces membrane invagination, and the oligomer is internalized in a vesicular structure. The mechanism of release from the vesicle could range from total dissolution of the vesicle to simple opening to the matrix compartment, with recovery of the bilayer.

membrane was completed, the pore would dissociate into subunits. If the rate of translocation is sufficiently rapid, such complexes might not be easily visualized by microscopic techniques. There has been a controversy in the peroxisomal literature regarding large pores. Mannaerts and colleagues have shown that peroxisomes, when isolated, have pores that allow small molecules such as nucleotides, to freely diffuse (van Veldhoven et al., 1983). On the other hand, there is evidence that a proton gradient exists across the peroxisomal membrane, at least in yeast (Bellion and Goodman, 1987; Nicolay et al., 1987). This would not be consistent with large pores that remain open. Perhaps the pores seen in vitro reflect the inappropriate assembly of protein transport units.

In contrast to these pore models, globular proteins may be imported by a mechanism analogous to endocytosis (Figure 10, *Membrane Internalization*). Thus, membrane vesicles may bud into the matrix of peroxisomes. In fact, although the peroxisome is called a unilamellar structure, internal membranes have been seen within peroxisomes in regenerating liver (Lüers et al., 1993) and in *S. cerevisiae* (V. Hines, personal communication). Moreover, the morphology of peroxisomes in two yeast peroxisomal assembly mutants termed PAS10 (van der Leij et al., 1992) and PAS22 (Elgersma et al., 1993) shows a large amount of internal membranous structures within the peroxisome. Internal membranes are also seen within the organelles in the human peroxisomal disease neonatal adrenoleukodystrophy (Motley et al., 1994). These mutants could represent defects in a membrane internalization pathway. If some peroxisomal proteins are indeed internalized, then a mechanism must exist for liberating them into the matrix compartment. Perhaps the general role of peroxisomes in phospholipid metabolism, or the general oxidizing environment of the matrix, is linked to this process. The extent of bilayer disruption causing release of contents (two extremes are illustrated in Fig. 10) is, of course, unknown.

Experiments are planned to determine whether endogenous proteins are imported as oligomers and to further dissect the mechanism of protein translocation across the peroxisomal membrane.

References

Aitchison, J. D., W. W. Murray, and R. A. Rachubinski. 1991. The carboxyl-terminal tripeptide Ala-Lys-Ile is essential for targeting *Candida tropicalis* trifunctional enzyme to yeast peroxisomes. *J. Biol. Chem.* 266:23197–23203.

America, T., J. Hageman, A. Guére, F. Rook, K. Archer, K. Keegstra, and P. Weisbeek. 1994. Methotrexate does not block import of a DHFR fusion

protein into chloroplasts. *Plant Mol. Biol.* 24:283–294.

Andersson, S., D. L. Davis, H. Dahlbäck, H. Jörnvall, and D. W. Russell. 1989. Cloning, structure, and expression of the mitochondrial cytochrome P-450 sterol 26-hydroxylase, a bile acid biosynthetic enzyme. *J. Biol. Chem.* 264:8222–8229.

Bellion, E., and J. M. Goodman. 1987. Proton ionophores prevent assembly of a peroxisomal protein. *Cell.* 48:165–173.

Blattner, J., B. Swinkels, H. Dörsam, T. Prospero, S. Subramani, and C. Clayton. 1992. Glycosome assembly in trypanosomes: Variations in the acceptable degeneracy of a COOH-terminal microbody targeting signal. *J. Cell Biol.* 119:1129–1136.

Blobel, G., and B. Dobberstein. 1975. Transfer of proteins across membranes I. Presence of proteolytically processed and unprocessed nascent immunoglobulin light chains on membrane-bound ribosomes of murine myeloma. *J. Cell Biol.* 67:835–851.

Bonner, W. M. 1978. Protein migration and accumulation in nuclei. *In* The Cell Nucleus. H. Busch, editor. Academic Press, New York. 97–148.

Brul, S., E. Weimer, A. Westerveld, A. Strijland, R. Wanders, A. Schram, H. Heymans, R. Schutgens, H. Van den Bosch, and J. Tager. 1988. Kinetics of the assembly of peroxisomes after fusion of complementary cell lines from patients with the cerebro-hepato-renal (Zellweger) syndrome and related disorders. *Biochem. Biophys. Res. Commun.* 152:1083–1089.

Chen, W.-J., and M. G. Douglas. 1987. The role of protein structure in the mitochondrial import pathway. Unfolding of mitochondrially bound precursors is required for membrane translocation. *J. Biol. Chem.* 262:15605–15609.

Cohen, G., W. Rapatz, and H. Ruis. 1988. Sequence of the *Saccharomyces cerevisiae* CTA1 gene and the amino acid sequence of catalase A derived from it. *Eur. J. Biochem.* 176:159–163.

de Duve, C. 1983. Microbodies in the living cell. *Sci. Am.* 248:74–84.

de Hoop, M., W. L. Holtman, and G. Ab. 1993. Human catalase is imported and assembled in peroxisomes of *Saccharomyces cerevisiae*. *Yeast.* 9:59–69.

de Hoop, M. J., and G. Ab. 1992. Import of proteins into peroxisomes and other microbodies. *Biochem. J.* 286:657–669.

Deshaies, R. J., B. D. Koch, M. Werner-Washburne, E. A. Craig, and R. Schekman. 1988. A subfamily of stress proteins facilitates translocation of secretory and mitochondrial precursor polypeptides. *Nature (Lond.).* 332:800–810.

Dingwell, C., S. V. Sharnick, and R. A. Laskey. 1982. A polypeptide domain that specifies migration of nucleoplasmin into the nucleus. *Cell.* 30:449–458.

Distel, B., S. J. Gould, B. T. Voorn, M. van der Berg, H. F. Tabak, and S. Subramani. 1992. The carboxyl-terminal tripeptide serine-lysine-leucine of firefly luciferase is necessary but not sufficient for peroxisomal import in yeast. *New Biol.* 4:157–165.

Eilers, M., and G. Schatz. 1986. Binding of a specific ligand inhibits import of a purified precursor protein into mitochondria. *Nature (Lond.).* 322:228–232.

Elgersma, Y., M. van den Berg, H. Tabak, and B. Distel. 1993. An efficient positive selection procedure for the isolation of peroxisomal import and peroxisomal assembly mutants by *Saccharomyces cerevisiae*. *Genetics.* 135:731–740.

Gietl, C. 1990. Glyoxysomal malate dehydrogenase from watermelon is synthesized with an amino-terminal transit peptide. *Proc. Natl. Acad. Sci. USA.* 87:5773–5777.

Goodman, J. M., L. J. Garrard, and M. T. McCammon. 1992. Structure and assembly of peroxisomal membrane proteins. *In* Membrane Biogenesis and Protein Targeting. W. Neupert and R. Lill, editors. Elsevier, Amsterdam. 209–220.

Goodman, J. M., C. W. Scott, P. N. Donahue, and J. P. Atherton. 1984. Alcohol oxidase assembles post-translationally into the peroxisome of Candida boidinii. *J. Biol Chem.* 259:8485–8493.

Gould, S. J., G.-A. Keller, and S. Subramani. 1987. Identification of a peroxisomal targeting signal at the carboxy terminus of firefly luciferase. *J. Cell Biol.* 105:2923–2931.

Gould, S. J., G.-A. Keller, and S. Subramani. 1988. Identification of peroxisomal targeting signals located at the carboxyl terminus of four peroxisomal proteins. *J. Cell Biol.* 107:897–905.

Gould, S. J., G.-A. Keller, N. Hosken, J. Wilkinson, and S. Subramani. 1989. A conserved tripeptide sorts proteins to peroxisomes. *J. Cell Biol.* 108:1657–1664.

Gould, S. J., G. A. Keller, M. Schneider, S. H. Howell, L. J. Garrard, J. M. Goodman, B. Distel, H. Tabak, and S. Subramani. 1990a. Peroxisomal protein import is conserved between yeast, plants, insects and mammals. *EMBO (Eur. Mol. Biol Organ.) J.* 9:85–90.

Gould, S. J., S. Krisans, G. A. Keller, and S. Subramani. 1990b. Antibodies directed against the peroxisomal targeting signal of firefly luciferase recognize multiple mammalian peroxisomal proteins. *J. Cell Biol.* 110:27–34.

Griffiths, G., A. McDowell, R. Back, and J. Dubochet. 1984. On the preparation of cryosections for immunocytochemistry. *J. Ultrastr. Res.* 89:65–78.

Hansen, H., T. Didion, A. Thiemann, M. Veenhuis, and R. Roggenkamp. 1992. Targeting sequences of the two major peroxisomal proteins in the methylotrophic yeast *Hansenula polymorpha*. *Mol. Gen. Genet.* 235:269–278.

Hartfield, C., A. McDowall, B. Loveland, and K. Fischer-Lindahl. 1991. Cellular location of thymus-leukemia (TL) antigen as shown by immunocryoultramicrotomy. *J. Electron Microsc. Technique.* 18:148–156.

Heinemann, P., and W. W. Just. 1992. Peroxisomal protein import: *in vivo* evidence for a novel translocation competent compartment. *FEBS (Fed. Eur. Biochem. Soc.) Lett.* 300:179–182.

Hendrick, J., and F.-U. Hartl. 1993. Molecular chaperone function of heat-shock proteins. *Annu. Rev. Biochem.* 62:349–384.

Hiltunen, K. J., B. Wenzel, A. Beyer, R. Erdmann, F. Fosså, and W. H. Kunau. 1992. Peroxisomal multifunctional beta-oxidation protein of *Saccharomyces cerevisiae*. Molecular analysis of the fox2 gene and gene product. *J. Biol Chem.* 267:6646–6653.

Kang, Y.-S., J. Kane, J. Kurjan, J. M. Stadel, and D. T. Tipper. 1990. Effects of expression of mammalian Gα and hybrid mammalian-yeast Gα proteins on the yeast pheromone response pathway. *Mol. Cell. Biol.* 10:2582–2590.

Keller, G. A., S. Krisans, S. J. Gould, J. M. Sommer, C. C. Wang, W. Schliebs, W. Kunau, S. Brody, and S. Subramani. 1991. Evolutionary conservation of a microbody targeting signal that targets proteins to peroxisomes, glyoxysomes, and glycosomes. *J. Cell Biol.* 114:893–904.

Kragler, F., A. Langeder, J. Raupachova, M. Binder, and A. Hartig. 1993. Two independent peroxisomal targeting signals in catalase A of *Saccharomyces cerevisiae*. *J. Cell Biol.* 120:665–673.

Kunkel, T. A., J. D. Roberts, and R. A. Zakour. 1987. Rapid and efficient site-specific mutagenesis without phenotypic selection. *Methods Enzymol.* 154:367–382.

Laemmli, U. K. 1970. Cleavage of structural proteins during the assembly of the head of bacteriophage T4. *Nature (Lond.).* 227:680–685.

Lazarow, P., and C. de Duve. 1973. The synthesis and turnover of rat liver peroxisomes. V. Intracellular pathway of catalase synthesis. *J. Cell Biol.* 59:507–524.

Lazarow, P., M. Robbi, F. Fujiki, and L. Wong. 1982. Biogenesis of peroxisomal proteins *in vivo* and *in vitro*. *Annu. N.Y. Acad. Sci.* 386:285–300.

Lazarow, P. B., and Y. Fujiki. 1985. Biogenesis of peroxisomes. *Annu. Rev. Cell Biol.* 1:489–530.

Leslie, A. G. 1990. Refined cyrstal structure of type III chloramphenicol acetyltransferase at 1.75 Å resolution. *J. Mol. Biol.* 213:167–186.

Lüers, G., T. Hashimoto, H. D. Fahimi, and A. Völkl. 1993. Biogenesis of peroxisomes: isolation and characterization of two distinct peroxisomal populations from normal and regenerating rat liver. *J. Cell Biol.* 121:1271–1280.

McCammon, M. T., M. Veenhuis, S. B. Trapp, and J. M. Goodman. 1990. Association of glyoxylate and beta-oxidation enzymes with peroxisomes of *Saccharomyces cerevisiae*. *J. Bacteriol.* 172:5816–5827.

McCammon, M. T., J. A. McNew, P. J. Willy, and J. M. Goodman. 1994. An internal region of the peroxisomal membrane protein PMP47 is essential for sorting to peroxisomes. *J. Cell Biol.* 124:915–925.

McNew, J. A., K. Sykes, and J. M. Goodman. 1993. Specific cross-linking of the proline isomerase cyclophilin to a non-proline-containing peptide. *Mol. Biol. Cell.* 4:223–232.

Middelkoop, E., E. Wiemer, D. Schoenmaker, A. Strijland, and J. Tager. 1993. Topology of catalase assembly in human fibroblasts. *Biochim. Biophys. Acta.* 1220:15–20.

Motley, A., E. Hetterna, B. Distel, and H. Tabak. 1994. Differential protein import deficiencies in human peroxisome assembly disorders. *J. Cell Biol.* 125:755–767.

Newmeyer, D., J. Lucocq, T. Burglin, and E. De Robertis. 1986. Assembly in vitro of nuclei active in nuclear protein transport: ATP is required for nucleoplasmin accumulation. *EMBO (Eur. Mol. Biol. Organ.) J.* 5:501–510.

Nicolay, K., M. Veenhuis, A. C. Douma, and W. Harder. 1987. A ^{31}P NMR study of the internal pH of yeast peroxisomes. *Arch. Microbiol.* 147:37–41.

Randall, L., and S. Hardy. 1986. Correlation of competence for export with lack of tertiary structure of the mature species: a study *in vivo* of maltose binding protein in *E. coli*. *Cell.* 46:921–928.

Sambrook, J., E. F. Fritsch, and T. Maniatis. 1989. Molecular Cloning: A Laboratory Manual. 2nd edition. Cold Spring Harbor Press, Cold Spring Harbor, NY.

Sanz, P., and D. I. Meyer. 1988. Signal recognition particle (SRP) stabilizes the translocation-competent conformation of pre-secretory proteins. *EMBO (Eur. Mol. Biol. Organ.) J.* 7:3553–3557.

Shaw, W., and A. Leslie, 1991. Cloramphenicol acetyltransferase. *Annu. Rev. Biophys. Chem.* 20:363–386.

Sikorski, R. S., and P. Hieter. 1989. A system of shuttle vectors and yeast host strains designed for efficient manipulation of DNA in *Saccharomyces cerevisiae*. *Genetics.* 122:19–27.

Silver, P. A. 1991. How proteins enter the nucleus. *Cell.* 64:489–497.

Small, G. M., L. J. Szabo, and P. B. Lazarow. 1988. Acyl-CoA oxidase contains two targeting sequences each of which can mediate protein import into peroxisomes. *EMBO (Eur. Mol. Biol. Organ.) J.* 7:1167–1173.

Swinkels, B. W., S. J. Gould, A. G. Bodnar, R. A. Rachubinski, and S. Subramani. 1991. A novel, cleavable peroxisomal targeting signal at the amino-terminus of the rat 3-ketoacyl-CoA thiolase. *EMBO (Eur. Mol. Biol. Organ.) J.* 10:3255–3262.

Swinkels, B. W., S. J. Gould, and S. Subramani. 1992. Targeting efficiencies of various permutations of the consensus C-terminal tripeptide peroxisomal

targeting signal. *FEBS (Fed. Eur. Biochem. Soc.) Lett.* 305:133–136.

Towbin, H., T. Staehelin, and J. Gordon. 1979. Electrophoretic transfer of proteins from polyacrylamide gels to nitrocellulose sheets: procedure and some applications. *Proc. Natl. Acad. Sci. USA.* 76:4350–4354.

Trumbly, R. 1992. Glucose repression in the yeast *Saccharomyces cerevisiae. Mol. Microbiol.* 6:15–21.

van der Leij, I., M. van den Berg, R. Boot, M. Franse, B. Distel, and H. F. Tabak. 1992. Isolation of peroxisome assembly mutants from *Saccharomyces cerevisiae* with different morphologies using a novel positive selection procedure. *J. Cell Biol.* 119:153–162.

van Veldhoven, P., L. Debeer, and G. Mannaerts. 1983. Water- and solute-accessible spaces of purified peroxisomes. Evidence that peroxisomes are permeable to NAD+. *Biochem. J.* 210:685–693.

Walton, P. A., S. J. Gould, R. A. Rachubinski, S. Subramani, and J. R. Feramisco. 1992. Transport of microinjected alcohol oxidase from *Pichia pastoris* into vesicles in mammalian cells: involvement of the peroxisomal targeting signal. *J. Cell Biol.* 118:499–508.

Waterham, H., V. Titorenko, G. Swaving, W. Harder, and M. Veenhuis. 1993. Peroxisomes in the methylotrophic yeast *Hansenula polymorpha* do not necessarily derive from pre-existing organelles. *EMBO (Eur. Mol. Biol. Organ.) J.* 12:4785–4794.

Wickner, W., A. Driessen, and F. U. Hartl. 1991. The enzymology of protein translocation across the *Escherichia coli* plasma membrane. *Annu. Rev. Biochem.* 60:101–124.